Highlights

This paper provides the first estimates of SGD to the Kuwait coastline in the Arabian Gulf. Seawater evaporation leads to density driven exchange between surface water and groundwater. Irrigation is likely a driver of SGD in Kuwait City and other arid urban megacities. Together these process may impact water quality in the receiving water body.

Anthropogenic and natural controls on coastal groundwater exchange in an arid region (Kuwait)

A. Fadlelmawla[a], M. Al-Senafy[a], and M.A. Charette[b]*

[a]*Water Resources Division, Kuwait Institute for Scientific Research*
[b]*Department of Marine Chemistry and Geochemistry, Woods Hole Oceanographic Institution*

Journal of Hydrology
Submitted on December 6, 2010
In revised form on June 15, 2011

*corresponding author
Mail Stop 25
266 Woods Hole Road
Woods Hole, MA 02543 USA
Email: mcharette@whoi.edu
Tel: 508-289-3205
Fax: 508-457-2193

SUMMARY

Submarine groundwater discharge (SGD) is an important, yet poorly understood component of the global water cycle. In arid climates, where overland flow is limited and often nonexistent, SGD may be the only significant vector for solute transport between land and sea. Here, we report the first direct estimates of SGD in Kuwait Bay and the Kuwait territorial waters of the Arabian Gulf, which were derived from an established approach involving a radium mass balance. The study consisted of three occupations of Kuwait Bay (October 2007; May 2008; October 2008) and a single transect in the Arabian Gulf in southern Kuwait (June 2008) as well as two groundwater sampling campaigns (January and October 2008). Dust was sometimes a non-negligible component of the Ra-budget; a large event in June 2008 accounted for up to 30% of the ^{226}Ra input to the Arabian Gulf transect. After accounting for additional sources and sinks, the radium mass balance in combination with a measured ^{226}Ra groundwater average of 170 dpm 100 L^{-1} resulted in submarine groundwater discharge rates that ranged from 1.1 to 2.8 x 10^7 m^3 d^{-1} (55 to 150 m^3 m^{-1} d^{-1}) for Kuwait Bay and 0.65 to 1.3 x 10^7 m^3 d^{-1} (65 to 125 m^3 m^{-1} d^{-1}) for the Arabian Gulf. In opposition to the seasonal precipitation pattern, lower SGD rates occurred in May/June while higher rates were observed in October. This phenomenon was explained by anthropogenic impacts on the local aquifer: groundwater levels in Kuwait City, hence hydraulic gradient towards the bay, are dominated by human-induced recharge due mainly to urban landscape irrigation. It was inferred that an additional driver of SGD was density-driven convection of groundwater within the surficial aquifer, which could explain unusually high Ra levels during October 2008 when bay water salinity was increased two fold due to intense evaporation.

***Keywords*:** Groundwater, Ocean, Salt water intrusion, Radium, Nutrients

Introduction

The flow of water from land to the oceans is a fundamental component of the global water cycle (Zektser and Dzhamalov, 2007). Most of the global flux of water across this boundary is attributed to streams and rivers, with the precipitation that recharges terrestrial aquifers contributing to the base flow of these streams (Baumgartner and Reichel, 1975). Only a few percent of the global land-to-sea water flux is generally attributed to submarine groundwater discharge (SGD) (Nace, 1967; Garrels and Mackenzie, 1971; Zektser and Dzhamalov, 2007). Recent evidence suggests that SGD may be substantially higher than previously thought, though much of this additional water flux may be as recirculated marine groundwater (Burnett et al., 2006). Regardless, understanding this component of the flux is required in order to close the water (and chemical flux) balance on local, regional, and global scales (Charette et al., 2008).

Despite the potential importance of land-to-sea groundwater flow, the magnitude and mechanism of this flux in various coastal settings are not well known. There are many reasons for this lack of understanding, though most often it is derived from limited information on the offshore hydrogeologic framework, such as the physical properties and hydraulic head in sub-seafloor aquifers. As a result, hydrologic models may be highly uncertain when used to predict groundwater flow (Mulligan and Charette, 2006). At the same time, both SGD and seawater intrusion may often occur as diffuse flow with exchange occurring through numerous small discharge/inflow points, which are difficult or impossible to locate and sample directly (Burnett et al., 2006).

Charette et al. (2008) discussed a rapidly growing database of SGD studies covering a wide range of climatological and hydrogeochemical conditions. However, there still is a general lack of investigations in arid regions. One may hypothesize that this is due to the idea that, because

groundwater recharge is generally low, SGD at the coast is likely to be non-existent. In one of the few examples, Weinstein et al. (2007) studied SGD along the coast of Israel where a confining unit that outcrops at the coastline was a conduit for low salinity groundwater input to the sea. Indeed, such confining units, which may recharge a great distance inland where precipitation rates are higher, may be the major delivery mechanism for SGD in dry climates. Surficial aquifers as a source of groundwater to the coast cannot be ruled out entirely; while recharge rates may be low, there is still the possibility of a small, but positive, hydraulic gradient that can drive SGD at the coast. This water, however, may be a mixture of saline porewater and meteoric groundwater (Swarzenski et al., 2006).

Coastal development in various forms has been shown to alter natural patterns in SGD. Steiglitz et al. (2007) reported that pier pilings installed through a shallow confining layer on Long Island (New York, USA) led to enhanced groundwater seepage. In a coastal Brazilian lagoon, Santos et al. (2008) found that agricultural irrigation and the associated drainage canals altered the natural flow of groundwater to the coast. Harvey and McCormick (2009) described the effects of the engineered Everglades (Florida, USA) wetland on groundwater-surface water interaction. Another factor that potentially influences SGD is the human induced groundwater recharge beneath seaside megacities (Yoshikoshi et al., 2009). In arid regions where natural recharge is minimum or absent, this type of artificial recharge, usually associated with irrigation of gardens and parks, significantly affects the levels of the groundwater and dominates their periodicity (Almedeij and Al-Ruwaih, 2006). Therefore, it could represent a new driving force for SGD.

Radium has been shown to be a useful indicator of SGD, which we define as advective flow of mixtures of fresh and brackish waters into the coastal zone (Moore, 1996; Rama and Moore,

1996; Krest et al., 2000; Charette et al., 2001). Two main factors make radium a useful tracer of SGD: (i) it is naturally enriched in brackish groundwater relative to seawater by several orders of magnitude, due to salinity-induced ion exchange and (ii) it behaves conservatively once released into marine waters. A radium excess in estuarine and coastal surface waters may be attributed to SGD, therefore estimation of SGD requires knowledge of surface water inventories as well as average Ra concentrations in groundwater near the expected point of discharge.

The existence of four naturally-occurring radium isotopes makes Ra also useful for quantifying multiple sources of SGD, such as fluid originating from confined versus surficial aquifers (Crotwell and Moore, 2003; Moore, 2003; Charette and Buesseler, 2004). This approach is made possible through two primary mechanisms. First, aquifers with different principal minerals or sediment types can have different relationships among uranium (^{238}U -> ^{226}Ra; ^{235}U -> ^{223}Ra) and thorium (^{232}Th -> ^{228}Ra -> ^{224}Ra) series isotopes. For example, aquifers with a predominance of carbonate minerals (e.g., karst) are enriched in U relative to Th, and therefore in U-series daughters (e.g., ^{226}Ra >> ^{228}Ra). Second, seawater circulation through an aquifer can result in sediments enriched in the shorter-lived isotopes and depleted in the longer-lived isotopes due to the relative differences in rates of ingrowth from their thorium parents (e.g., ^{228}Ra >> ^{226}Ra; Hancock and Murray, 1996). This phenomenon can be used to estimate groundwater residence times.

Here, we report the use of radium isotopes, for the first time under extreme arid conditions, to quantify the source and flux of submarine groundwater discharge in Kuwait Bay, a shallow embayment that is linked to the Arabian Gulf. We also examine direct SGD to the Arabian Gulf from an offshore radium transect in the southern portion of the country. Seasonal and interannual

SGD patterns were also studied. Lastly, short-lived Ra isotopes were used to estimate water mass ages for Kuwait Bay, which approximate bay flushing rates.

Study Area

Extremely high temperatures, as well as short mild winters, long days, low humidity and generally dry conditions are the main climatic characteristics of the study area (Grealish et al., 2001). Meteorological data for the period 1962 – 1989 indicates that the air temperature ranged between 7°C and 39.3°C. The annual mean precipitation is 105.6 mm with high inter-annual variability (the lowest mean was 23 mm in 1960 and the highest was 242 mm in 1976). Precipitation occurs mostly during December and January with monthly averages of 24.1 mm and 18.2 mm, respectively (Al-Sulaimi et al., 1997). A key feature of the arid weather of Kuwait is the common and intense dust storm. This phenomenon, which is more frequent during summer, results in a significant contribution of sedimentary debris to the bay (Foda et al., 1985). Such debris can present a significant source for radium that should be taken into account when constructing the radium budget for the bay. Foda et al. (1985) developed a numerical model to simulate the penetration of dust storms originating from the Iraqi territories over the northern parts of the Arabian Gulf. They estimated that such storms would yield dust sedimentation rates of 0.8 mm yr^{-1}, which is substantially higher than dust fallout in most seas of the world.

Marine waters that border the country of Kuwait include Kuwait Bay and the Arabian Gulf (Fig. 1). The bay itself has an average depth of ~8 m and covers a surface area of 880 km^2. The depth distribution is not uniform–the northern bay is characterized by wide tidal flats (< 2 m) and a relatively narrow sill in the south. The central part of the bay has a 10-20 m trough that shallows progressively from east to west. The bay exchanges freely with the Arabian Gulf mainly through tides, which have a maximum amplitude of 3.5 to 4 m. At the bay/gulf boundary to the north, the Khawr Abd Allah estuary is a potential external water source, though recent damming of the estuary has led to greatly reduced flow.

Being an incursion of the Arabian Gulf into the Arabian Peninsula landmass, Kuwait Bay is thus a part of the groundwater discharge zone along the coastline of the peninsula. The Ghar Formation of the Kuwait Group borders the southern rim of the Kuwait Bay. The formation can be divided into an unconfined Upper Aquifer and semi-confined Lower Aquifer, separated by an aquitard formed by a zone of alternating sandy mudstone and muddy sandstone within this sequence. Along the northern periphery of the bay, younger Lower Fars Formation of the Kuwait Group, which conformably overlies the Ghar Formation and is richer in carbonate with the occasional presence of evaporates, is exposed. The saturated thickness of the Kuwait Group ranges between 60 and 210 m. Transmissivity of this formation ranges from 170 to 375 m^2 d^{-1} due to thickness variations as well as the degree of cementation. These values were obtained through pumping tests.

The potentiometric head contours of the Kuwait Group aquifers around Kuwait Bay further show that the groundwater flow along the southern coast of the bay is northeasterly to the Arabian Gulf and to Kuwait Bay and southeasterly along the northern coast of the bay (Fig. 1), consistent with the general idea of Kuwait Bay being a part of the regional discharge zone. From this data, we divided the coastline into 14 unique segments and performed a Darcy's Law based estimate of groundwater flow to the coast, which totaled 44,800 m^3 d^{-1} (Appendix 1). Total dissolved solids (TDS) in the surficial aquifer surrounding the bay are generally high (ranging between 10,000 to 20,000 mg L^{-1}). To the south of the bay, groundwater becomes more saline as one approaches the coastal areas from the interior of the country. In the northern part of the bay, a zone of less saline water (~1000 mg L^{-1}) exists very near the coastal zone.

Groundwater levels beneath the urban areas bordering the bay have been on the rise for the last three decades (Al-Rashed and Sherif, 2001), extending to depths of 1-2 meters from the

ground surface for most of Kuwait City. This is mostly due to the interruption of the natural hydrological cycle by human induced recharge from water distribution system leakages and excessive watering of landscaping. Of relevance to this study is the potential enhancement of SGD due to elevated groundwater gradients and the impacts of this human-induced recharge on the variation of groundwater levels, hence SGD. Almedeij and Al-Ruwaih (2006) indeed showed that fluctuations in groundwater level in the urban areas of Kuwait is controlled by water consumption and not regional precipitation patterns.

Finally, Kuwait Bay is probably the most distinct and important feature of the Kuwaiti coast. With high productivity and its long shoreline, the bay plays a significant role in the socioeconomics of Kuwait. In the last decade, the bay has suffered recurring red tides. These conditions call for sound management practices to ensure that an ecological balance is maintained within the bay. A prerequisite of such a management is the identification and quantification of the various natural and anthropogenic sources that comprise the Kuwait Bay nutrient budget. This study has been carried out to obtain such knowledge on one of the significant elements of the water budget of the bay: non-point source inputs via SGD.

Methods

Four surface water and five groundwater sampling excursions were carried out during this study. Within Kuwait Bay, 10-14 sampling stations were occupied throughout the bay for each trip (Fig. 1). A shore perpendicular transect (n=9 stations) was chosen to examine direct SGD from Kuwait to the Arabian Gulf. Groundwater samples were collected at 28 wells bordering the bay and gulf. The total depth of the wells ranged between 20 and 50 m according to the topography, with screened submerged intervals of 12 to 20 m.

Surface water samples (100 L) were filtered and collected into barrels or containers with spigots. Filling these containers was achieved by deckboard pump. Samples were processed through MnO_2-coated acrylic fiber (Moore and Reid, 1973) at a flow rate of < 1 L min^{-1}. Groundwater samples (50 L) were collected using a submersible pump and processed through Mn-fiber as described above. To ensure representative sampling, the wells were purged until pH, electrical conductivity, dissolved oxygen and temperature were stable prior to sample collection. These *in situ* measurements were conducted using Jenway portable meters (370 and 470).

Back in the laboratory, ^{224}Ra and ^{223}Ra were quantified by alpha counting on a delayed coincidence counter (Moore and Arnold, 1996). Radium-224 was calibrated by a ^{232}Th solution with daughters in equilibrium transferred onto Mn oxide fiber and analyzed in the same geometry as samples. The short-lived Ra-isotopes were decay corrected to the time of collection and for activity supported by their parent isotopes (^{228}Th and ^{227}Ac); the latter correction was made by reanalyzing the samples after ~6 half-lives of ^{224}Ra and ^{223}Ra, respectively, had elapsed. Analysis of ^{226}Ra was performed by radon equilibration in a sealed, evacuated glass column using a Durridge RAD7 alpha counting instrument (Peterson et al., 2009). Radium-226 standards were prepared from a NIST-certified solution transferred onto Mn oxide fibers. Radium-228 was

analyzed using a Canberra Ge gamma spectrometer. The Mn-fiber samples were compressed into a disk geometry (65-mm diameter, 5-mm thick) inside of a metal canister. ^{228}Ra was quantified from a weighted average of counts from the 338 keV and 911 keV peaks of ^{228}Ac. The Ge detector was standardized by counting U–Th ore DL-1a (Canadian Certified Reference Materials Project) prepared in the same geometry as the compressed fibers.

Results and Discussion

Surface water Ra distribution

Results from the surface water and groundwater analyses are presented as a table in the appendix. Radium activities in surface water were generally 2-3 times higher in the October periods when compared with the May period (Fig. 2). Radium-226, for example, ranged from 9.4-21.7 dpm 100 L^{-1} (avg = 15 dpm 100 L^{-1}) in October 2007 and from 18.0-30.1 dpm 100 L^{-1} (avg = 25 dpm 100 L^{-1}) in October 2008. Activities for May 2008 were 4.5-11.1 dpm 100 L^{-1} (avg = 7.3 dpm 100 L^{-1}). Given that Indian Ocean ^{226}Ra values are rarely < 7-8 dpm 100 L^{-1} (Ostlund et al., 1987), some of our lower activity samples may be indicative of a problem with Mn cartridge collection efficiency. Distributions of radium-226 in the bay generally decrease with increasing distance from the nearest coastal land mass suggesting that the radium source to the bay is coastally-derived (Fig. 2; r^2 = 0.22, 0.24 for Oct-07 and May-08, respectively). There is a no correlation with distance from land during October 2008; we contend that this is due to increased residence time of the bay leading to a more homogeneous radium distribution.

The short-lived Ra isotopes and ^{228}Ra generally tracked the ^{226}Ra distribution pattern within the bay and variation between time periods. For the October 2007 period, ^{223}Ra ranged from 0.39-0.82 dpm 100 L^{-1} with an average of 0.57 dpm 100 L^{-1}. Radium-224 spanned 3.3-12 dpm 100 L^{-1} with an average of 7.0 dpm 100 L^{-1}. Radium-228 ranged from 20-40 dpm 100 L^{-1} with an average of 32 dpm 100 L^{-1}. In May 2008, ^{223}Ra ranged from 0.40-1.7 dpm 100 L^{-1} with an average of 0.74 dpm 100 L^{-1}. Radium-224 spanned 1.1-15 dpm 100 L^{-1} with an average of 5.8 dpm 100 L^{-1}. Radium-228 ranged from 5.2-22 dpm 100 L^{-1} with an average of 12 dpm 100 L^{-1}. Lastly, for October 2008, ^{223}Ra ranged from 0.28-1.4 dpm 100 L^{-1} with an average of 0.95 dpm

252 100 L^{-1}. Radium-224 spanned 9.8-22 dpm 100 L^{-1} with an average of 16 dpm 100 L^{-1}. Radium-
253 228 ranged from 36-69 dpm 100 L^{-1} with an average of 50 dpm 100 L^{-1}.

254 Bay water electrical conductivity (EC), which is used here as a proxy for salinity, also varied
255 during these periods and tended to increase in concert with radium activity (Fig. 3a). Because
256 October is the end of the dry season, evaporation is a major factor for the higher EC. Due to its
257 conservative behavior in seawater, ^{226}Ra follows a similar trend. In order to determine if there is
258 true variation in the radium inputs between sampling periods, we normalized the radium data to
259 the EC at station KBS01 during October 2007, which we assume to be representative of the
260 Arabian Gulf endmember that exchanges with the bay. The EC normalized averages for the three
261 time periods are 14, 12, and 22 dpm 100 L^{-1} (Fig. 3b). This analysis reveals that evaporation
262 alone cannot fully explain the seasonal variation and that there must be very real differences
263 between Ra inputs to the bay among the three time periods. In particular, October inputs are on
264 average higher than May, which is surprising given that this is the end of the summer dry period.

265 During October 2008, a water sample was collected from Khawr Abd Allah, the former
266 mouth of the Tigris-Euphrates River system that is at present a drowned river estuary. The ^{226}Ra
267 activity was 22 dpm 100 L^{-1} (EC normalized = 28 dpm 100 L^{-1}). The EC measured at this
268 location indistinguishable from the outer bay samples to the south. Al-Ghadban and El-Sammak
269 (2005) suggest that, due to prevailing currents, flow from this system is not likely to impact
270 Kuwait Bay proper. Combined with the fact that the natural flow of the Tigris-Euphrates system
271 has been greatly diminished over the years by damming (Jones et al., 2008), we do not expect
272 that this estuary is a major source of radium to the bay.

273 For the late June 2008 offshore transect southeast of the city of Ahmadi, ^{226}Ra activities
274 ranged from 11-19 dpm 100 L^{-1} with an average of 15 dpm 100 L^{-1}. When normalized to EC, this

range becomes 14-24 dpm 100 L^{-1} (avg = 19 dpm 100 L^{-1}). Radium-228 ranged from 13-30 dpm 100 L^{-1} (avg = 21 dpm 100 L^{-1}). These activities are similar to the October 2008 values from Kuwait Bay, which is surprising given that they are from an open coastline and not an embayment with (presumably) longer water residence times. However, all samples were collected within 8 km of shore, close enough such that an SGD-derived Ra signal could persist without significant dilution by low Ra offshore water. While the short-lived isotopes generally decreased with distance from shore (^{223}Ra range = 0.06-0.52 dpm 100 L^{-1}; ^{224}Ra range = 0.40-6.1 dpm 100 L^{-1}), the long-lived Ra isotopes displayed the opposite pattern. This could be explained a one or more of the following: (1) wind driven upwelling of bottom water enriched in ^{223}Ra and ^{224}Ra due to contact with bottom sediments, (2) onshore advection of an older coastal water plume that has its long-lived Ra signature intact but has lost ^{223}Ra and ^{224}Ra due to decay, (3) an offshore groundwater source, or (4) radium input from intense dust storms, which is quantified in a later section of the paper.

Groundwater Ra distribution

Groundwater ^{226}Ra activities ranged from 15-1200 dpm 100 L^{-1} and averaged 170 ± 260 dpm 100 L^{-1}. The average ^{223}Ra, ^{224}Ra, and ^{228}Ra activities were 110 ± 300, 370 ± 900, and 450 ± 500 dpm 100 L^{-1}, respectively. The large variation as indicated by the high standard deviations of the averages is not atypical for Ra in groundwater, because a wide range of biogeochemical processes control the concentration of Ra in the dissolved phase of subsurface systems (Gonneea et al., 2008). There was no apparent correlation between groundwater radium and EC or any other property (i.e., redox potential, dissolved oxygen, major ions). In addition, there was no relationship between Ra activity and depth within the aquifer, though this is not entirely

surprising given that most wells were screened within the top 30 m (i.e. approximately the top third of the aquifer) of the unconfined aquifer (Kuwait Group). Groundwater $^{228}Ra/^{226}Ra$ ratios were generally within the range of 1-5 with an average of 3.3 (Fig. 4a). These ratios are typical for the sands and sandstones that characterize the aquifer formation, supporting the idea of a geologic control on groundwater radium, in agreement with a recent study on Ra isotopes in a North Carolina (USA) aquifer (Vinson et al., 2009). The lack of $^{228}Ra/^{226}Ra$ activity ratios $<<1$ precludes significant leakage from the underlying confined aquifer into the surficial aquifer.

Radium isotopic ratios can therefore provide insight into the potential sources of submarine groundwater discharge to a coastal system. In the case of the short-lived Ra isotopes (^{223}Ra, ^{224}Ra), they may be used to quantify water mass ages, which in turn may be used to evaluate the flushing time of a coastal embayment. For the ratio of $^{228}Ra/^{226}Ra$, the surface water samples fall within the range of 1-3 (Fig. 4b). If we assume the offshore $^{228}Ra/^{226}Ra$ activity ratio is similar to that of the northwestern Indian Ocean (activity ratio = 1.0), then the Kuwait Bay data fall on a mixing line between the offshore and average groundwater endmember described above. This supports the idea that we have captured the likely SGD endmember that led to the radium enrichments within the Kuwait Bay.

Radium mass balance for Kuwait coastal waters

Though the aquifers that intersect the coastline of Kuwait Bay do not contain purely fresh groundwater (low TDS), the water table is above sea level and is hydraulically connected to the bay (Fig. 1). These two characteristics indicate the SGD is occurring in this region. Because radium is less particle reactive under high ionic strength (high TDS), we expect that the groundwater in this region should have elevated radium concentration. Additionally, aquifer

materials provide an unlimited renewable source of radium via the decay of their particle bound thorium parent isotopes.

The radium activities observed in the Kuwait Bay are within the range of those observed for many studies where SGD has been deemed an important vector for the delivery of dissolved chemicals to the coastal zone. The combined range for ^{226}Ra for the three time periods of 4.5-30 dpm 100 L^{-1} is comparable to the activities observed by Moore (1996) in the South Atlantic Bight (USA) where volumetrically, SGD was 40% of the river discharge to the coast. Ratios of $^{228}Ra/^{226}Ra$ are often indicative of the aquifer mineralogy from which the SGD originated (Moore, 2003; Charette and Buesseler, 2004). Ratios for the Kuwait Bay averaged 2.0, which is typical for coastal regions with SGD originating from aluminosilicate sediments (Charette et al., 2008). Though we do not have data for the central Arabian Gulf, $^{228}Ra/^{226}Ra$ ratios of 1-1.5 would make a logical endmember that explains the groundwater and seawater ratios of 3.8 and 2.0, respectively. The absence of $^{228}Ra/^{226}Ra$ ratios <1 is notable in that such values would indicate that a groundwater source from karst formations (U enriched, Th depleted) may be present. However, this does not appear to be the case for the Kuwait Bay. This observation allows us to rule out major groundwater contributions to the bay from the Lower Kuwait Group and Dammam Formation, the shallowest lithological units with a preponderance of carbonate minerals (Mukhopadhyay et al., 1996).

Diffuse fluxes such as SGD are difficult to quantify. Thus, a "flux by difference" approach is required, whereby all quantifiable (and non-negligible) radium fluxes are subtracted from the flux required to support the inventory of the isotope with the residual flux being attributed to SGD (Charette et al., 2008). Besides SGD, there are five main natural pathways for enrichment or removal of these nuclides in the coastal ocean that must be considered. Potential sources

include riverine discharge, diffusion from low permeability bottom sediments, and SGD. In this desert environment where dust storms are intense and prevalent during certain times of year, aeolian inputs must also be considered. Removal or loss terms include exchange with open ocean waters and radioactive decay. Scavenging/biological uptake, which can affect the budget, is another removal process. For Ra, this process is assumed negligible relative to other removal terms in the coastal ocean. Of special note for the Kuwait Bay are potential anthropogenic Ra sources including wastewater discharge and desalination brine. In the case of wastewater, there are no known domestic sources of Ra, making this an unlikely pathway for Ra input to the bay. On the other hand, the desalination brine should be significantly enriched in Ra regardless of purification process (reverse osmosis or distillation). However, since bay water is the source of the desalination feed water, the net effect on the radium budget should be negligible.

A water sample from the Khawr Abd Allah estuary was collected during this study. Though it displayed a slightly elevated ^{226}Ra activity relative to the bay average, the lack of significant flow (Jones et al. 2008) from this potential river input into the Kuwait Bay precludes it as a meaningful source. Additionally, the river estuary discharges directly into the Arabian Gulf and is therefore not a direct source of Ra to the bay. This leaves SGD, dust, and diffusion from sediments as the only major sources. If we use radium-226 (or ^{228}Ra) as our SGD tracer, exchange with the Arabian Gulf through tidal and wind driven mixing is the lone removal process we need to account for (decay of these isotopes is negligible on the time scale of mixing in the bay). The box model in equation form is as follows:

$$^{226}Ra_{SGD} = \underbrace{\left| \frac{\left(^{226}Ra_{KB} - ^{226}Ra_{AG}\right) \times V_{KB}}{\tau_{KB}} \right|}_{F_{Mix}} - F_{Sed} - F_{Dust} \qquad (1)$$

where $^{226}Ra_{KB}$ is the average concentration of ^{226}Ra within the Kuwait Bay, $^{226}Ra_{AG}$ is the ^{226}Ra concentration of the Arabian Gulf waters that enter the Kuwait Bay through tidal exchange, V_{KB} and τ_{KB} are the volume and residence time of water in the Kuwait Bay, respectively. These terms are solved to determine the loss via mixing (F_{Mix}). The determination of τ_{KB} using Ra isotopes is discussed in a later section.

The middle term (F_{Sed}) is the diffusive flux of Ra from the sediments (irrespective of SGD). A simple test determining the upper limit magnitude of this flux involves the measurement of the top 5 cm inventory of total ^{226}Ra in the bay sediments. Then, by assuming: (1) that the surface bound inventory is a fixed fraction of the total (~40% for fine-grained sediments: Rama and Moore, 1996; Gonneea et al., 2008), (2) all of this Ra is available for diffusion, and (3) a literature value for solute diffusion from fine-grained sediments, a diffusive flux can be estimated. Most studies find that F_{Sed} is usually a small component of the overall Ra mass balance (<5%; Charette et al., 2001). For this study, we were unable to quantify the Ra inventory in the surface sediments, hence, we used the values from Waquoit Bay, MA, USA (Charette et al., 2001) and scaled it to the bottom surface area of the Kuwait Bay. This comparison is appropriate because of the similarity in sediment mineralogy between the two locations.

The final term (F_{Dust}) is the input of Ra from atmospherically transported dust, which represents a constant but non-steady state source term. The majority of the dust input occurs via dust storms, which take place typically between June and July, associated with the strong northwesterly winds that characterize the monsoon season (Foda et al., 1985). This input may be calculated from an estimate of dust inputs over the bay and the amount of radium that is surface bound and therefore available for desorption once deposited in the saline bay water.

Water residence time for Kuwait coastal waters derived from radium isotopes

The short-lived radium isotope distributions can provide information on the ages (or residence time) of water masses in the coastal ocean. To calculate the age of the Kuwait Bay water (τ_{KB}) relative to the time when it contacted firstly the coastal water, one can use an approach based on the ratio of $^{224}Ra/^{228}Ra$ in groundwater (the main source of Ra to the system) relative to that found in a given water parcel (Moore et al., 2006):

$$F^{224}Ra = I^{224}Ra\left(\lambda_{224} + \frac{1}{\tau_{KB}}\right) \quad (2)$$

where F ^{224}Ra is the total flux (dpm m^{-2} d^{-1}) of ^{224}Ra to the system, I ^{224}Ra is its inventory (dpm m^{-2}), λ_{224} is its decay constant (d^{-1}), and τ_{KB} is the apparent age (d) of water in Kuwait Bay. A similar equation can be written for ^{228}Ra; however, because its half-life is 5.75 years, the effect of decay can be ignored.

$$F^{228}Ra = I^{228}Ra\left(\frac{1}{\tau_{KB}}\right) \quad (3)$$

Dividing equation 2 by equation 3 and rearranging:

$$\tau_{KB} = \frac{\left[F\left(^{224}Ra/^{228}Ra\right) - I\left(^{224}Ra/^{228}Ra\right)\right]}{I\left(^{224}Ra/^{228}Ra\right)\lambda_{224}} \quad (4)$$

In this case F(^{224}Ra/^{228}Ra) is the ^{224}Ra/^{228}Ra activity ratio of the input into the system and I(^{224}Ra/^{228}Ra) is the ^{224}Ra/^{228}Ra ratio of the seawater. The application of this model requires knowledge of the ^{224}Ra/^{228}Ra ratio of input and allows for continuous input within the bay or along the transect. In our case, this value was determined by measuring the ratio in groundwater collected from the coastal monitoring wells. For example, in May 2008 at station KBS007 west of Kuwait City (Figs. 1 and 5), the value of F(^{224}Ra/^{228}Ra) was 0.85 and the value of I(^{224}Ra/^{228}Ra) was 0.85. Given λ_{224} of 0.189 d^{-1}, equation (4) yields a water age for this station of 4.3 days. This approach is useful on time scales appropriate to the ^{224}Ra half-life (up to ~25 days). Radium-223 and its decay constant may be substituted in equations (3) and (4) in cases where the flushing times are expected to be significantly longer (up to ~2 months). This approach was used for the October 2007 dataset as the ^{224}Ra activities had an unacceptably large uncertainty due to a delay in analysis from the time of collection.

We used this approach to compute the water mass ages for the three Kuwait Bay sampling periods. The distributions of Ra-derived ages are presented in Fig. 5. In general, ages were higher in the central bay and off Kuwait City than those at the northern and eastern boundary stations. This pattern is consistent with the hydrodynamic circulation model for the Kuwait Bay developed by Rakha et al. (2007), which revealed two gyres within the central bay that could lead to enhanced residence times. In terms of the seasonal averages, the mean age of bay water was higher in the dry season (16 and 20 days for October 2007 and 2008, respectively). The May 2008 average was 13 days. In support of these data is the fact that τ_{KB} increased with increasing average Kuwait Bay conductivity since longer residence times would lead to higher evaporation. In addition, the longer residence times observed for October 2008 support our earlier observation that ^{226}Ra was well mixed throughout the bay and did not correspond to station proximity to the

coast. Ages for the Arabian Gulf transect ranged from 5-10 days at the inner 2 stations and 32 days at the farthest offshore station (8 km); the average for the transect was 16 days.

The right hand side of equation (1) is solved and the residual radium flux (excess of inputs-outputs) is assumed to be the ^{226}Ra flux due to SGD ($^{226}Ra_{SGD}$) for Kuwait Bay. The groundwater ^{226}Ra concentration (GW_{Ra}) that supplied the excess Ra flux to the bay (an average of all coastal monitoring wells) is the remaining term required to quantify the groundwater flux (F_{SGD}):

$$F_{SGD} = \frac{^{226}Ra_{SGD}}{GW_{Ra}} \quad (5)$$

In equation (1), the excess radium inventory of the bay is the difference between the average bay concentration and the offshore water that exchanges with the bay due to tidal mixing. Our sampling grid did not extend far enough offshore to capture the true Arabian Gulf endmember. For ^{226}Ra, we assume that this is equal to the northwestern Indian Ocean surface water average of 8.0 dpm 100 L^{-1} (GEOSECS Station 416; Ostlund et al., 1987). Radium-228 was not quantified in the surface water of GEOSECS Station 416. Therefore, we applied the ^{228}Ra/^{226}Ra ratio from Station 446 of ~1.5 to arrive at a ^{228}Ra endmember of 12 dpm 100 L^{-1}. Using the October 2008 sampling period as an example (Table 1), the excess ^{226}Ra inventory is 9.5 x 10^{11} dpm. With an average residence time of 19.8 days, the excess ^{226}Ra flux is 4.8 x 10^{10} dpm d^{-1}.

The ^{226}Ra flux from bottom sediment porewater diffusion is estimated at 3.5 x 10^{7} dpm d^{-1} using sediment ^{226}Ra production rates from Charette et al. (2001). This ^{226}Ra source is negligible as it represents approximately 0.1% of the excess ^{226}Ra flux. For evaluating F_{Dust}, we obtained monthly settled dust data from the Al-Shuwaikh area (Fig. 6). According to the analysis by Foda

et al. (1985), this monitoring station is located within a "mean dust turbidity" region (Fig. 7 whereas the Kuwait Bay and the offshore region is located in the "moderate" to "high" dust turbidity area; therefore, these estimates may represent lower limit values. Given that the flushing time of the bay is less than 1 month, we assume that any dust-derived Ra must originate from a fairly recent event. For October 2007, the dust flux was 0.52 g m^{-2} d^{-1}. With equal distribution over the bay, the total flux is equal to 4.6 x 10^8 g d^{-1}. Moore (1996) reported desorbable ^{226}Ra in fine grained river sediment equal to ~2 dpm g^{-1}; Gonneea et al. (2008) measured the desorbable ^{226}Ra in aluminosilicate sands at 5 x 10^{-3} dpm g^{-1}. Using these values as upper and lower limit bounds we can constrain the possible contribution of ^{226}Ra from settled dust in the Kuwait Bay at 2.3-920 x 10^6 dpm d^{-1}. This represents approximately 0.01-4% of the excess ^{226}Ra flux for October 2007. In contrast, dust may account for as much as 30% of the excess radium in the Arabian Gulf transect due to a significant dust event in June 2008 (7 g m^{-2} d^{-1}).

Submarine groundwater discharge derived from radium isotopes: seasonal cycling and driving forces

From the average ^{226}Ra in groundwater (n=57) of 170 dpm 100 L^{-1} and equation (5), we derive an SGD flux of 2.8 x 10^7 m^3 d^{-1}. We can also solve these equations using ^{228}Ra and arrive at an SGD of 2.4 x 10^7 m^3 d^{-1} for the same time period. When normalized to the Kuwait Bay shoreline length of 1.9 x 10^5 m, we estimate SGD at 150 and 130 m^3 m^{-1} d^{-1} for ^{226}Ra and ^{228}Ra, respectively. Overall, our estimates of SGD in the Kuwait Bay and the Arabian Gulf transect range from 1.1 to 2.8 x 10^7 m^3 d^{-1} (55 to 150 m^3 m^{-1} d^{-1}; Table 1). The fluxes were similar for October 2007 and May 2008 but they were a factor of ~2 higher for October 2008.

These results, which are inverse to the seasonal rainfall pattern, may be explained by groundwater level variation due to water consumption patterns. Almedeij and Al-Ruwaih (2006) have shown that groundwater levels in Kuwait City, hence gradient towards the bay, are dominated by human-induced recharge mainly due to urban landscape irrigation (Fig. 8). This artificial recharge follows a pattern similar to temperature (with about three months lag) rather than rainfall (Fig. 9). As illustrated in Fig. 9, the highest land-bay gradient, hence SGD (if driven by this process), would be expected in September and October. Conversely, the lowest gradients occur from March to mid May, in good agreement with the lower average Ra activities in the bay observed in May 2008. Hamdan and Mukhopadhyay (1991) provide further evidence of the significance of urban recharge in the overall discharge to the sea. Through numerical modeling, they estimated the man-made recharge to be more than 85% of the total recharge received by the aquifer within the Kuwait City premises.

Given similar water levels, artificial urban groundwater recharge cannot fully explain the difference between the two October periods. Another possibility is that intensive evaporation within the bay led to density driven advective exchange of radium-enriched porewater within the bay in October 2008. Given that porewater conductivity within the Kuwait Bay is likely a long-term average of EC within the bay, a large increase in bay EC would therefore result in an unstable density gradient that may lead to gravitational convection (Rapaglia and Bokuniewicz, 2009). Moore and Wilson (2005) reported similar density-driven SGD on the eastern U.S. continental shelf, though the exchange processes they reported were caused by a temperature gradient rather than EC as hypothesized here. The high fluxes derived from Ra isotopes as compared with the Darcy's Law estimate (4.5×10^4 m^3 d^{-1}) suggest that this may be the more dominant process in driving exchange through the aquifer.

499 The average radium-derived SGD for Kuwait Bay falls within the median SGD for a number
500 of locations a wide range of geologic and climatologic characteristics (Fig. 10). This is surprising
501 for such an arid climate, and significantly higher than rates reported by Swarzenski et al. (2006)
502 and Weinstein et al. (2007) for Dor Beach, Israel (5.0-7.1 m^3 m^{-1} d^{-1}). Large-scale urban
503 irrigation at Kuwait City and suburban areas can partially explain these differences. In addition,
504 the Israeli site was a beach-scale study (focused on the inner ~100 m of the coastline) that likely
505 did not account for SGD occurrence at a significant distance beyond the intertidal zone, an
506 observation noted by Charette et al. (2008) in a comparison of a large number of local vs.
507 regional scale studies.

508

509

Conclusions

This paper provides the first estimates of submarine groundwater discharge to Kuwait Bay and the Kuwait coastline in the Arabian Gulf. Using radium as a tracer for groundwater, estimates of SGD rates ranged from 1.1 to 2.8 x 10^7 m^3 d^{-1} (55 to 150 m^3 m^{-1} d^{-1}) for Kuwait Bay and 0.65 to 1.3 x 10^7 m^3 d^{-1} (65 to 125 m^3 m^{-1} d^{-1}) for the Arabian Gulf. The following observations are the major findings from this study:

(1) Dust storms greater than ~5 g m^{-2} d^{-1} have the potential to add significant quantities of radium to Kuwait coastal waters. This source must be accounted for when using radium isotopes as a tracer of SGD in this and similar environments.

(2) Seawater evaporation during hot and dry periods results in hypersaline conditions within Kuwait Bay, which in turn may lead to density driven exchange between surface water and groundwater within the shallow surficial aquifer.

(3) Irrigation of Kuwait City and suburban areas has led to a ~1-4 m increase in aquifer water levels beneath the city over the past two decades. The increase is likely a driver of SGD in Kuwait City and other urban megacities in arid regions.

We surmise that, as water rise problems are typically accompanied by high nitrate and potentially other contaminants of ecological concern, this process may impact water quality in the receiving water body.

Acknowledgements

This work was funded by a grant from the Kuwait Foundation for the Advancement of Sciences. M.A.C. was also supported by a grant from the National Science Foundation (OCE-0751525). Radium analyses were carried out by A. Vengosh and his research group at Duke University. Assistance in the field was provided by many capable technical support staff at the Kuwait Institute for Scientific Research. The authors benefited by discussions with H. Bokuniewicz on ideas relating to density driven flow. This manuscript was improved greatly by comments from four anonymous reviewers.

References

Al-Ghadban, A.N., and A. El-Sammak. (2005). Sources distribution and composition of the suspended sediments, Kuwait Bay, Northern Arabian Gulf. *Journal of Arid Environments*, **60:** 647-661.

Almedeij, J., and F. Al-Ruwaih. (2006). Periodic behavior of groundwater level fluctuations in residential areas. *Journal of Hydrology*, **328**: 677-684.

Al-Rashed, M.F. and M.M. Sherif. (2001) Hydrogeological Aspects of Groundwater Drainage of the Urban Areas in Kuwait City. *Hydrological Processes*, **15**: 777-795.

Al-Sulaimi J., F. I. Khalaf and A. Mukhopadhyay. (1997). Geomorphological Analysis of Paleo Drainage Systems and their Environmental Implications in the Desert of Kuwait. *Environmental Geology,* **29**: 95-111.

Baumgartner, A. and E. Reichel (1975). The world water balance: Mean annual global, continental and maritime precipitation, evaporation and runoff. Elsevier, Amsterdam, p. 179.

Boehm, A.B., Paytan, A., Shellenbarger, G.G. and Davis, K.A., (2006). Composition and flux of groundwater from a California beach aquifer: Implications for nutrient supply to the surf zone. *Continental Shelf Research*, **26:** 269-282.

Burnett, W. C., P. K. Aggarwal, A. Aureli, H. Bokuniewicz, J. E. Cable, M. A. Charette, E. Kontar, S. Krupa, K. M. Kulkarni, A. Loveless, W. S. Moore, J. A. Oberdorfer, J. Oliveira, N. Ozyurt, P. Povinec, A. M. G. Privitera, R. Rajar, R. T. Ramessur, J. Scholten, T. Stieglitz, M. Taniguchi, and J. V. Turner. (2006). Quantifying submarine

groundwater discharge in the coastal zone via multiple methods. *Science of the Total Environment* **367:** 498-543.

Burnett, W. C. (2002). Assessing methodologies for measuring groundwater discharge to the ocean. *EOS* **83:** 117-123.

Burnett, W. C. and H. Dulaiova. (2006). Radon as a tracer of submarine groundwater discharge into a boat basin in Donnalucata, Sicily. *Continental Shelf Research* **26:** 862-873.

Cable, J. E., W. C. Burnett, J. P. Chanton, and G. L. Weatherly. (1996). Estimating groundwater discharge into the northeastern Gulf of Mexico using radon-222. *Earth and Planetary Science Letters* **144:** 591-604.

Charette, M. A., and K. O. Buesseler. (2004). Submarine groundwater discharge of nutrients and copper to an urban subestuary of Chesapeake bay (Elizabeth River). *Limnology and Oceanography* **49:** 376-385.

Charette, M. A., K. O. Buesseler, and J. E. Andrews. (2001). Utility of radium isotopes for evaluating the input and transport of groundwater-derived nitrogen to a Cape Cod estuary. *Limnology and Oceanography* **46:** 465-470.

Charette, M.A., W.S. Moore, and W.C. Burnett. (2008) Uranium- and thorium-series nuclides as tracers of submarine groundwater discharge. In: S. Krishnaswami and J.K. Cochran (Editors) "U-Th Series Nuclides in Aquatic Systems", Series: Radioactivity in the Environment, Elsevier.

Crotwell, A. M., and W. S. Moore. (2003). Nutrient and radium fluxes from submarine groundwater discharge to Port Royal Sound, South Carolina. *Aquatic Geochemistry* **9:** 191-208.

Dulaiova, H., W. C. Burnett, J. P. Chanton, W. S. Moore, H. J. Bokuniewicz, M. A. Charette, and E. Sholkovitz. (2006a). Assessment of groundwater discharges into West Neck Bay, New York, via natural tracers. *Continental Shelf Research* **26:** 1971-1983.

Dulaiova, H., W. C. Burnett, G. Wattayakorn, and P. Sojisuporn. (2006b). Are groundwater inputs into river-dominated areas important? The Chao Phraya River – Gulf of Thailand. *Limnology and Oceanography* **51:** 2232-2247.

Foda, M. A. F. I. Khalaf, A. S. Al-Kadi. (1985). Estimation of dust fallout rates in the northern Arabian Gulf. *Sedimentology*, **32**: 595-603.

Garrels, R. M., and F. T. Mackenzie. (1971). Evolution of Sedimentary Rocks. W.W. Norton and Company, New York, 397 pp.

Gonneea, M.E., P. Morris, H. Dulaiova, and M.A. Charette. (2008). New perspectives on radium behavior within a subterranean estuary. *Marine Chemistry*, **109**: 250-267.

Grealish G., S. Omar and M. Quinn. (1998). Affected Area Soil Survey-Assessing Damage Magnitude and Recovery of the Terrestrial Eco-system - Follow-up of Natural and Induced Desert Recovery. KISR Report FA 015C.

Hancock, G. J., and A. S. Murray. (1996). Source and distribution of dissolved radium in the Bega River estuary, Southeastern Australia. *Earth and Planetary Science Letters,* **138:** 145-155.

Harvey, J.W. and McCormick, P.V., 2009. Groundwater's significance to changing hydrology, water chemistry, and biological communities of a floodplain ecosystem, Everglades, South Florida, USA. *Hydrogeology Journal*, **17**(1): 185-201.

Hwang, D. W., G. B. Kim, Y. W. Lee, and H. S. Yang. (2005a). Estimating submarine inputs of groundwater and nutrients to a coastal bay using radium isotopes. *Marine Chemistry*, **96:** 61-71.

Hwang, D. W., Y. W. Lee, and G. Kim. (2005b). Large submarine groundwater discharge and benthic eutrophication in Bangdu Bay on volcanic Jeju Island, Korea. *Limnology and Oceanography*, **50:** 1393-1403.

Jones, C., M. Sultan, E. Yan, A. Milewski, M. Hussein, A. Al-Dousari, S. Al-Kaisy, R. Becker. (2008). Hydrologic impacts of engineering projects on the Tigris-Euphrates system and its marshlands, *Journal of Hydrology*, **353**, 59-75.

Kelly, R. P., and S. B. Moran. (2002). Seasonal changes in groundwater input to a well-mixed estuary estimated using radium isotopes and implications for coastal nutrient budgets. *Limnology and Oceanography*, **47:** 1796-1807.

Kim, G., J. W. Ryu, H. S. Yang, and S. T. Yun. (2005). Submarine groundwater discharge (SGD) into the Yellow Sea revealed by Ra-228 and Ra-226 isotopes: Implications for global silicate fluxes. *Earth and Planetary Science Letters*, **237:** 156-166.

Krest, J. M., W. S. Moore, L. R. Gardner, and J. T. Morris. (2000). Marsh nutrient export supplied by groundwater discharge: Evidence from radium measurements. *Global Biogeochemical Cycles*, **14:** 167-176.

Moore, W.S., and D.F. Reid, (1973). Extraction of radium from natural waters using manganese-impregnated acrylic fibers. *Journal of Geophysical Research*, **90**: 6983-6994.

Moore, W.S., and R. Arnold, 1996. Measurement of ^{223}Ra and ^{224}Ra in coastal waters using a delayed coincidence counter. *Journal of Geophysical Research*, **101**: 1321-1329.

626 Moore, W. S. (1996). Large groundwater inputs to coastal waters revealed by Ra-226
627 enrichments. *Nature,* **380:** 612-614.

628 Moore, W. S. (1997). High fluxes of radium and barium from the mouth of the Ganges-
629 Brahmaputra river during low river discharge suggest a large groundwater source. *Earth*
630 *and Planetary Science Letters,* **150:** 141-150.

631 Moore, W. S. (2003). Sources and fluxes of submarine groundwater discharge delineated by
632 radium isotopes. *Biogeochemistry,* **66:** 75-93.

633 Moore, W. S. (2006). Radium isotopes as tracers of submarine groundwater discharge in Sicily.
634 *Continental Shelf Research,* **26:** 852-861.

635 Moore, W. S., J. O. Blanton, and S. Joye. (2006). Estimates of Flushing Times, Submarine
636 Groundwater Discharge, and Nutrient Fluxes to Okatee River, South Carolina. *Journal of*
637 *Geophysical Research-Oceans,* **111:** doi: 10.1029/2005JC003041.

638 Mulligan, A. E., and M. A. Charette. (2006). Intercomparison of submarine groundwater
639 discharge estimates from a sandy unconfined aquifer. *Journal of Hydrology* **327:** 411-
640 425.

641 Mukhopadhyay, A., J. Al-Sulaimi, E. Al-Awadi, F. Al-Ruwaih. (1996). An overview of the
642 Tertiary geology and hydrogeology of the northern part of the Arabian Gulf region with
643 special reference to Kuwait, *Earth-Science Reviews*, **40:** 259-295.

644 Mukhopadhyay, A., A. Al-Haddad, M. Al-Otaibi, and M. Al-Senafy. (2007). Occurrence of
645 hydrogen sulfide in the ground water of Kuwait. *Environmental Geology,* **52:** 1151-1161.

646 Nace, R.L. (1967) Are we running out of water? U.S. Geological Survey Circular 556, 53 pp.

Ostlund, H.G., H. Craig, W.S. Broecker, and D. Spencer. (1987). GEOSECS Atlantic, Pacific, and Indian Ocean Expeditions Volume 7: Shorebased Data and Graphics. 200 pp.

Peterson, R.N., Burnett, W.C., Dimova, N. and Santos, I.R., 2009. Comparison of measurement methods for radium-226 on manganese-fiber. *Limnology and Oceanography-Methods*, **7**: 196-205.

Purkl, S., and A. Eisenhauer. (2004). Determination of radium isotopes and Rn-222 in a groundwater affected coastal area of the Baltic Sea and the underlying sub-sea floor aquifer. *Marine Chemistry* **87:** 137-149.

Rakha, K., K. Al-Banaa, A. Al-Ragum, and F. Al-Hulail. (2007). Hydrodynamic Model for Kuwait Bay. 32nd Congress of IAHR, Paper 193, July 2007 Venice, Italy.

Rama, and W. S. Moore. (1996). Using the radium quartet for evaluating groundwater input and water exchange in salt marshes. *Geochimica et Cosmochimica Acta* **60:** 4645-4652.

Rapaglia, J. P., and H. J. Bokuniewicz. (2009). The effect of groundwater advection on salinity in pore waters of permeable sediments. *Limnology and Oceanography*, **54**: 630–643.

Riedl, R. J., N. Huang, and R. Machan. (1972). The subtidal pump: a mechanism of interstitial water exchange by wave action. *Marine Biology* **13:** 210-221.

Santos, I.R. et al., 2008. Tracing anthropogenically driven groundwater discharge into a coastal lagoon from southern Brazil. *Journal of Hydrology*, **353**(3-4): 275-293.

Stieglitz, T.C., Rapaglia, J. and Krupa, S.C., 2007. An effect of pier pilings on nearshore submarine groundwater discharge from a (partially) confined aquifer. *Estuaries and Coasts*, **30**(3): 543-550.

Swarzenski, P. W., W. C. Burnett, W. J. Greenwood, B. Herut, R. Peterson, N. Dimova, Y. Shalem, Y. Yechieli, and Y. Weinstein (2006). Combined time-series resistivity and geochemical tracer techniques to examine submarine groundwater discharge at Dor Beach, Israel, *Geophysical Research Letters*, **33**, doi:10.1029/2006GL028282.

Vinson, D.S., A. Vengosh, D. Hirschfeld, G. S. Dwyer. (2009). Relationships between radium and radon occurrence and hydrochemistry in fresh groundwater from fractured crystalline rocks, North Carolina (USA), *Chemical Geology*, **260**: 159-171.

Weinstein, Y., W. C. Burnett, P. W. Swarzenski, Y. Shalem, Y. Yechieli, and B. Herut (2007). Role of aquifer heterogeneity in fresh groundwater discharge and seawater recycling: An example from the Carmel coast, Israel, *Journal of Geophysical Research*, **112**, doi:10.1029/2007JC004112.

Yoshikoshi, A. et al., 2009. Hydro-environmental changes and their influence on the subsurface environment in the context of urban development. *Science of the Total Environment*, **407**(9): 3105-3111.

Zektser, I. S. (2000). Groundwater and the Environment: Applications for the Global Community. Lewis Publishers. Boca Raton, 175 pp.

Zekster, I. S., R. G. Dzhamalov. (2007). Submarine Groundwater. CRC Press, 512 Pp.

683

684

Table 1. Summary of box model assumptions and SGD fluxes for Kuwait Bay and direct discharge to the Arabian Gulf.

Term	Oct-07		May-08		Oct-08		Jun-08 (Arabian Gulf)	
	^{226}Ra	^{228}Ra	^{226}Ra	^{228}Ra	^{226}Ra	^{228}Ra	^{226}Ra	^{228}Ra
Kuwait Bay Ra Avg. (dpm 100 L^{-1})	13.7	31.3	12.1	20.9	21.6	43.1	15.5	21.3
Arabian Gulf Ra (dpm 100 L^{-1})	8.0	12.0	8.0	12.0	8.0	12.0	8.0	12.0
Kuwait Bay Age (days)*	16	16	13	13	19	19	16	16
Kuwait Bay Volume (m^3)	7.0E+09	7.0E+09	7.0E+09	7.0E+09	7.0E+09	7.0E+09	7.0E+09	7.0E+09
Kuwait Bay Area (m^2)	8.8E+08	8.8E+08	8.8E+08	8.8E+08	8.8E+08	8.8E+08	8.0E+08	8.0E+08
Shoreline Length (m)	1.9E+05	1.9E+05	1.9E+05	1.9E+05	1.9E+05	1.9E+05	1.0E+05	1.0E+05
Gross Ra Flux (dpm d^{-1})	2.4E+10	8.2E+10	2.2E+10	4.8E+10	5.0E+10	1.2E+11	3.3E+10	4.1E+10
Sediment Diffusion (dpm d^{-1})**	3.5E+07	3.5E+07	3.5E+07	3.5E+07	3.5E+07	3.5E+07	3.5E+07	3.5E+07
Desorption from Dustfall (dpm d^{-1})**	9.2E+08	9.2E+08	3.3E+09	9.2E+08	2.1E+09	2.1E+09	1.1E+10	1.1E+10
Net Ra Flux (dpm d^{-1})	2.3E+10	8.1E+10	1.9E+10	4.7E+10	4.8E+10	1.1E+11	2.1E+10	2.9E+10
Groundwater Ra Avg. (dpm 100 L^{-1})	171	451	171	451	171	451	171	451
SGD (m^3 d^{-1})	1.4E+07	1.8E+07	1.1E+07	1.0E+07	2.8E+07	2.5E+07	1.3E+07	6.5E+06
Shoreline-normalized SGD (m^3 m^{-1} d^{-1})	71	93	57	54	147	130	125	65

*Oct-07 age determined from ^{223}Ra/^{228}Ra.

685 **Assumed ^{228}Ra/^{226}Ra activity ratio of 1.

686

687

688

689

690

691

692

693

694

695

696

697

698

699

700

701

702

703

Figures

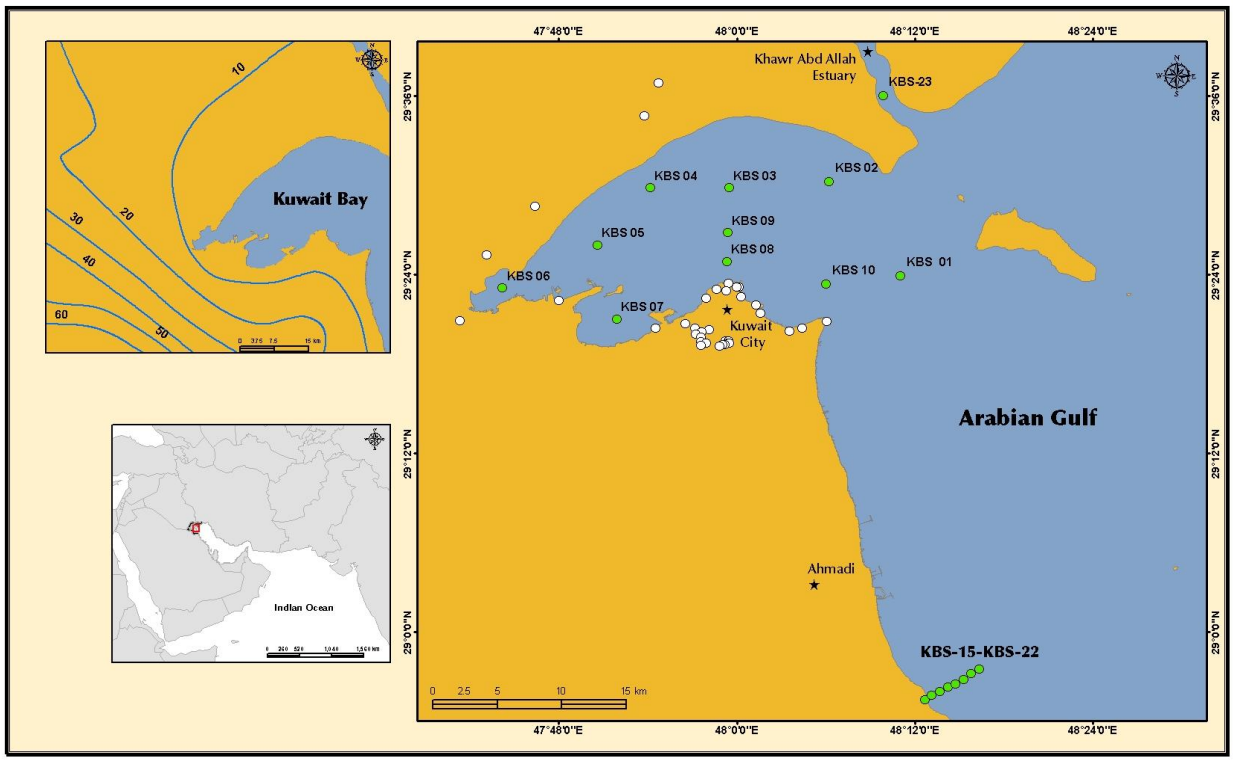

Figure 1. Potentiometric contours (in meters) for the Kuwait Group aquifer (top left). Station locations for surface water (green circles) and groundwater (white circles) sampling (right). Groundwater station IDs can be found in the data summary table. The Arabian Gulf transect station IDs begin with KBS15 nearshore and increase to KBS22 for the most offshore location.

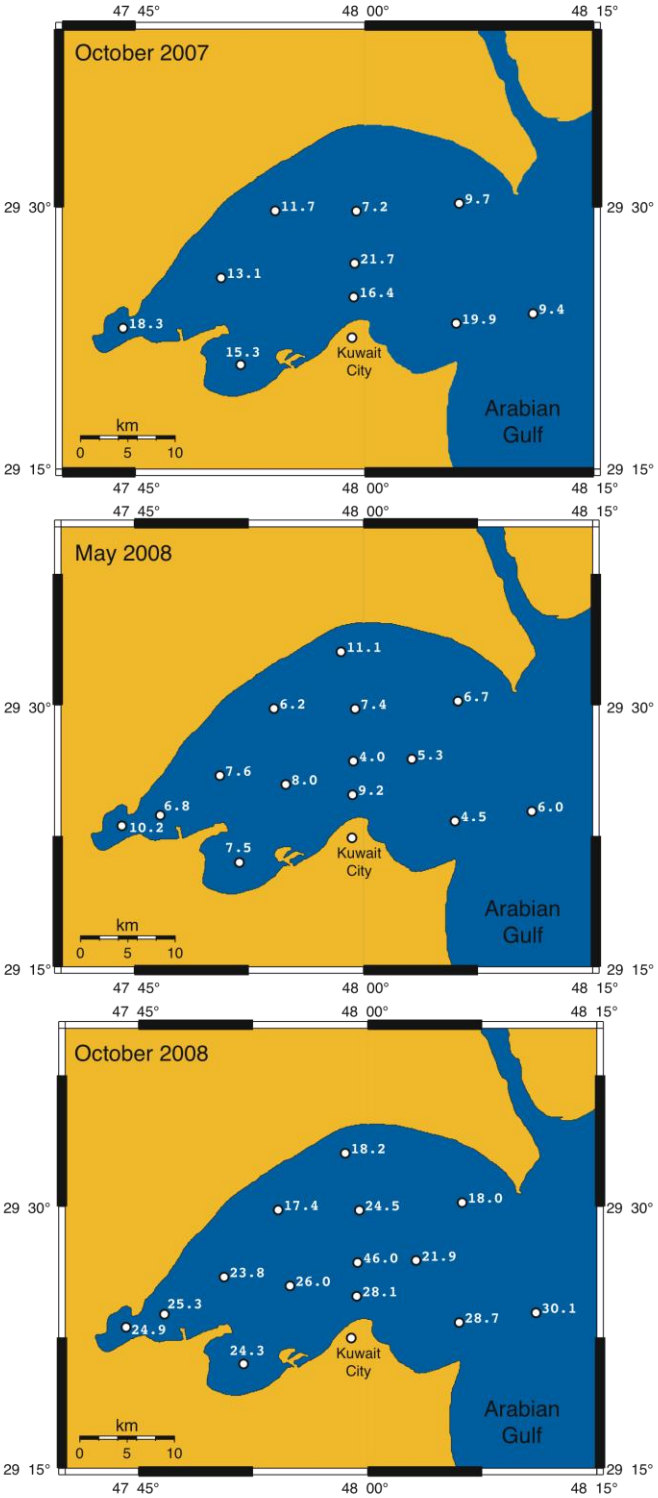

Figure 2. ^{226}Ra activities in Kuwait Bay for the three sampling periods. Units are dpm 100 L^{-1}.

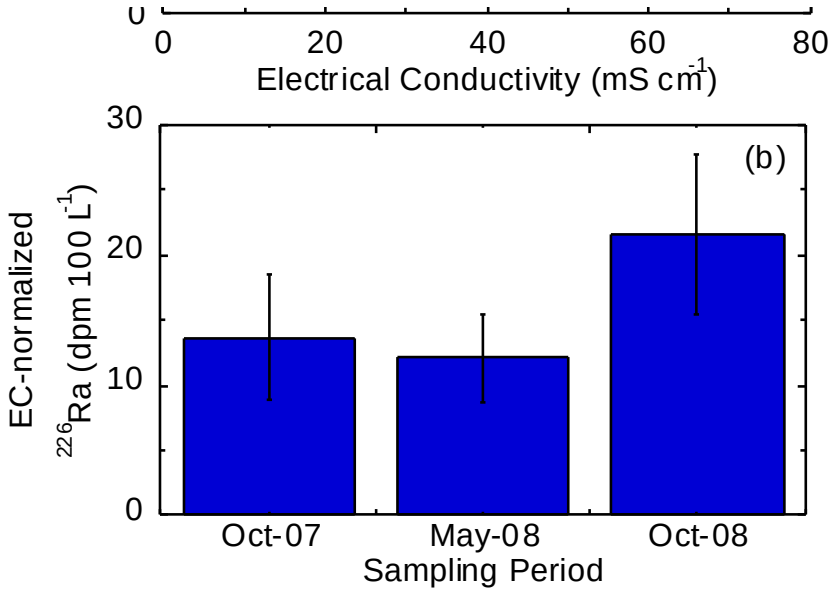

Figure 3. (a) Radium-226 vs. electrical conductivity (EC) for all four sampling periods including the offshore transect within the Arabian Gulf. (b) Average electrical conductivity (EC) normalized ^{226}Ra for the three Kuwait Bay sampling periods.

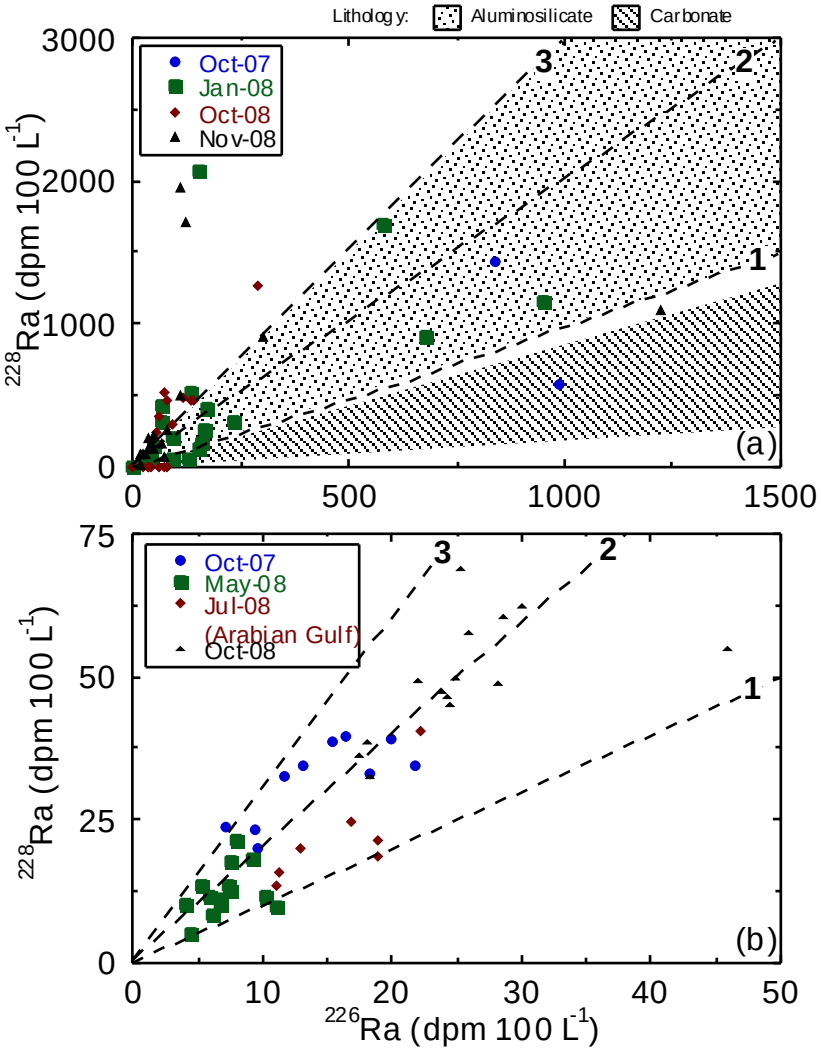

Figure 4. (a) Long-lived radium isotopes from groundwater sampling. Dashed lines indicate the ^{228}Ra/^{226}Ra activity ratio (AR). Shaded areas highlight activity ratios indicative of aluminosilicate vs. carbonate lithology (key at top). (b) Long-lived radium isotopes from surface water sampling (including the Arabian Gulf transect). Dashed lines indicate the ^{228}Ra/^{226}Ra activity ratio (AR).

744

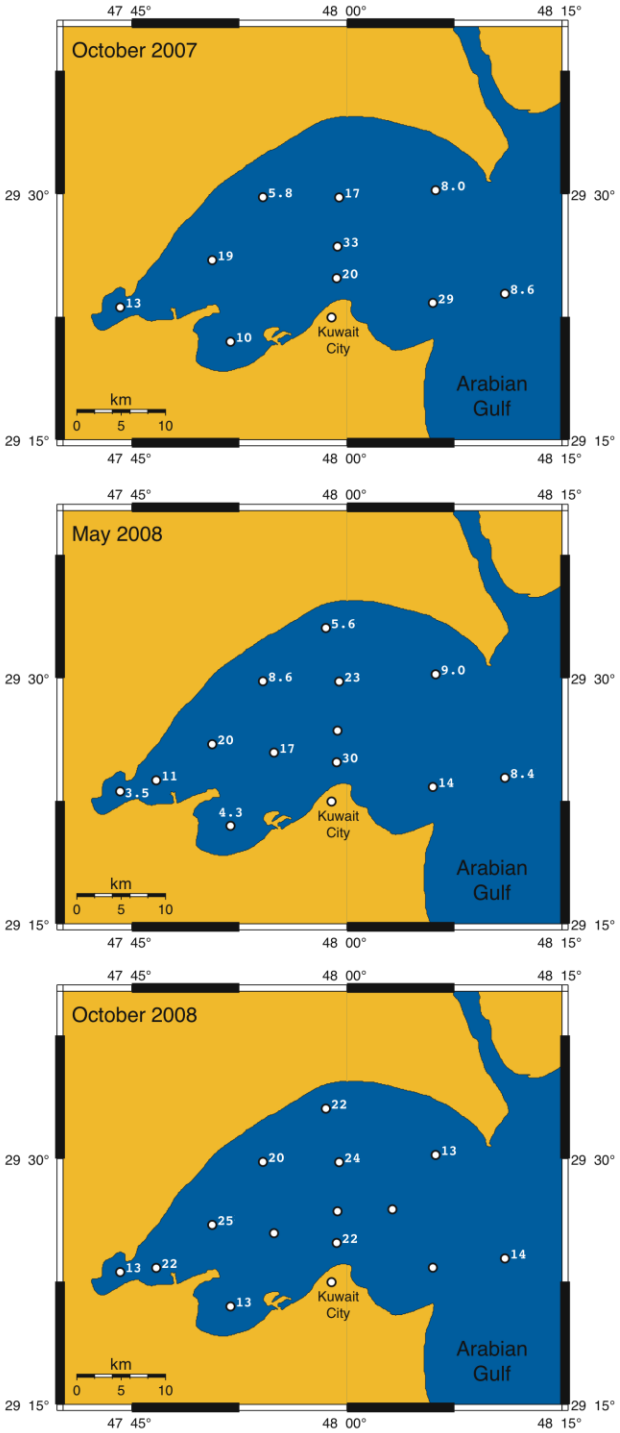

745

746

747 **Figure 5. Distribution of short-lived Ra-derived water mass ages (in units of days) for**
748 **Kuwait Bay.**

749

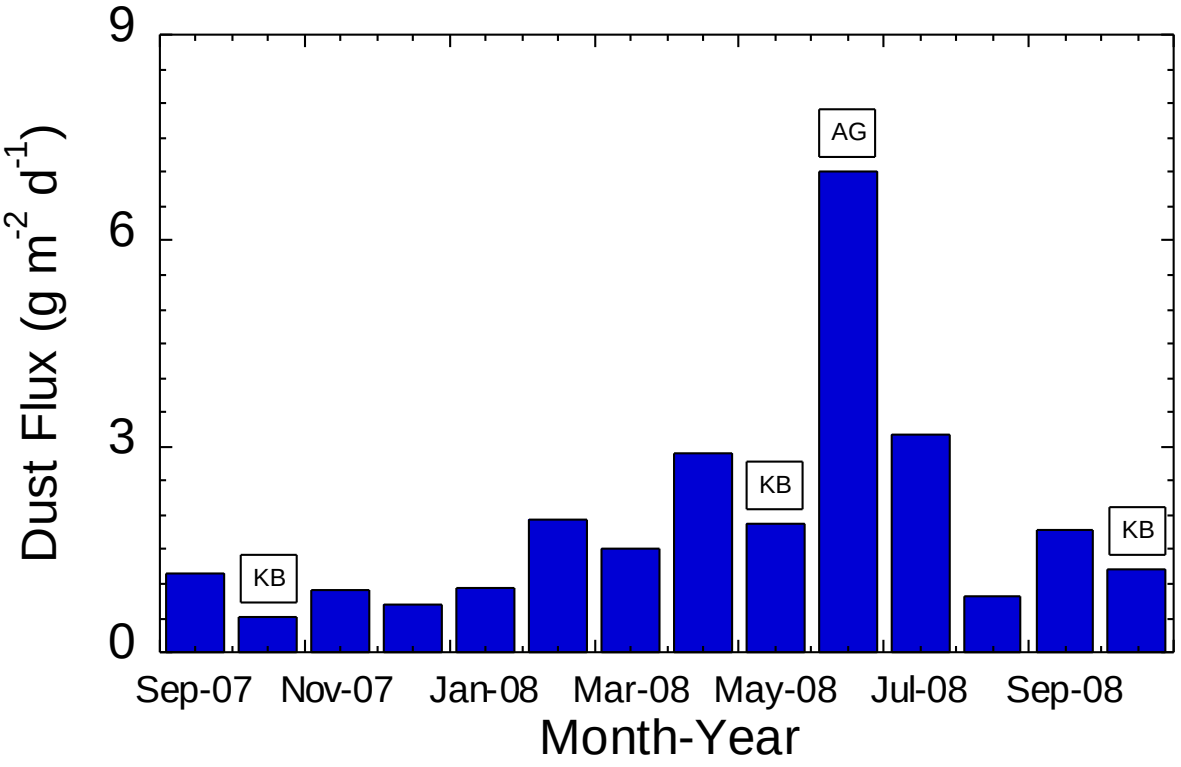

Figure 6. Monthly average dust fallout for coastal Kuwait from September 2007 through October 2008. Also shown are the Kuwait Bay (KB) and Arabian Gulf (AG) transect sampling periods.

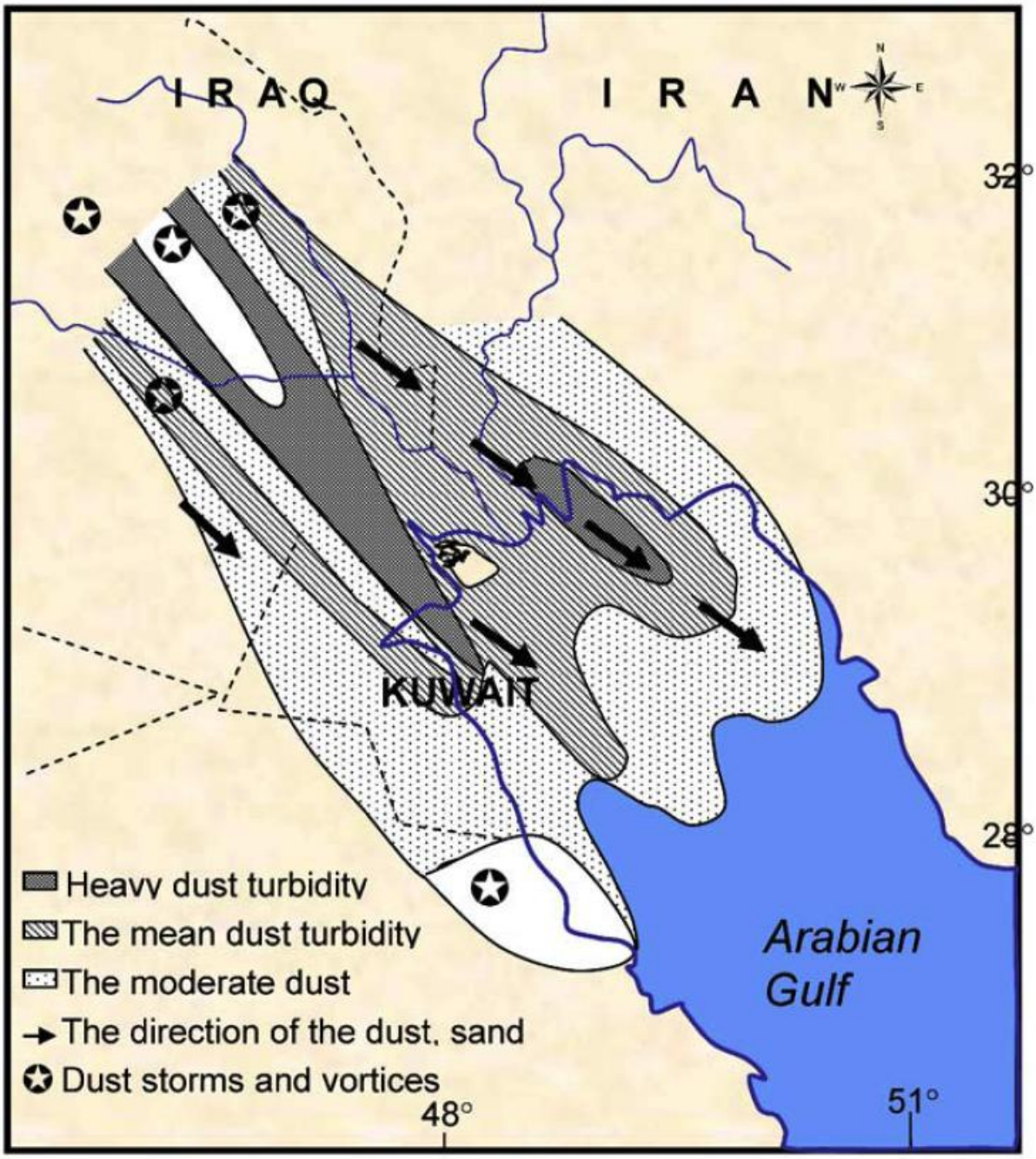

Figure 7. Dust storm direction and intensity over Kuwait Bay and the Arabian Gulf (reprinted from Al-Ghadban and E-Sammak, 2005).

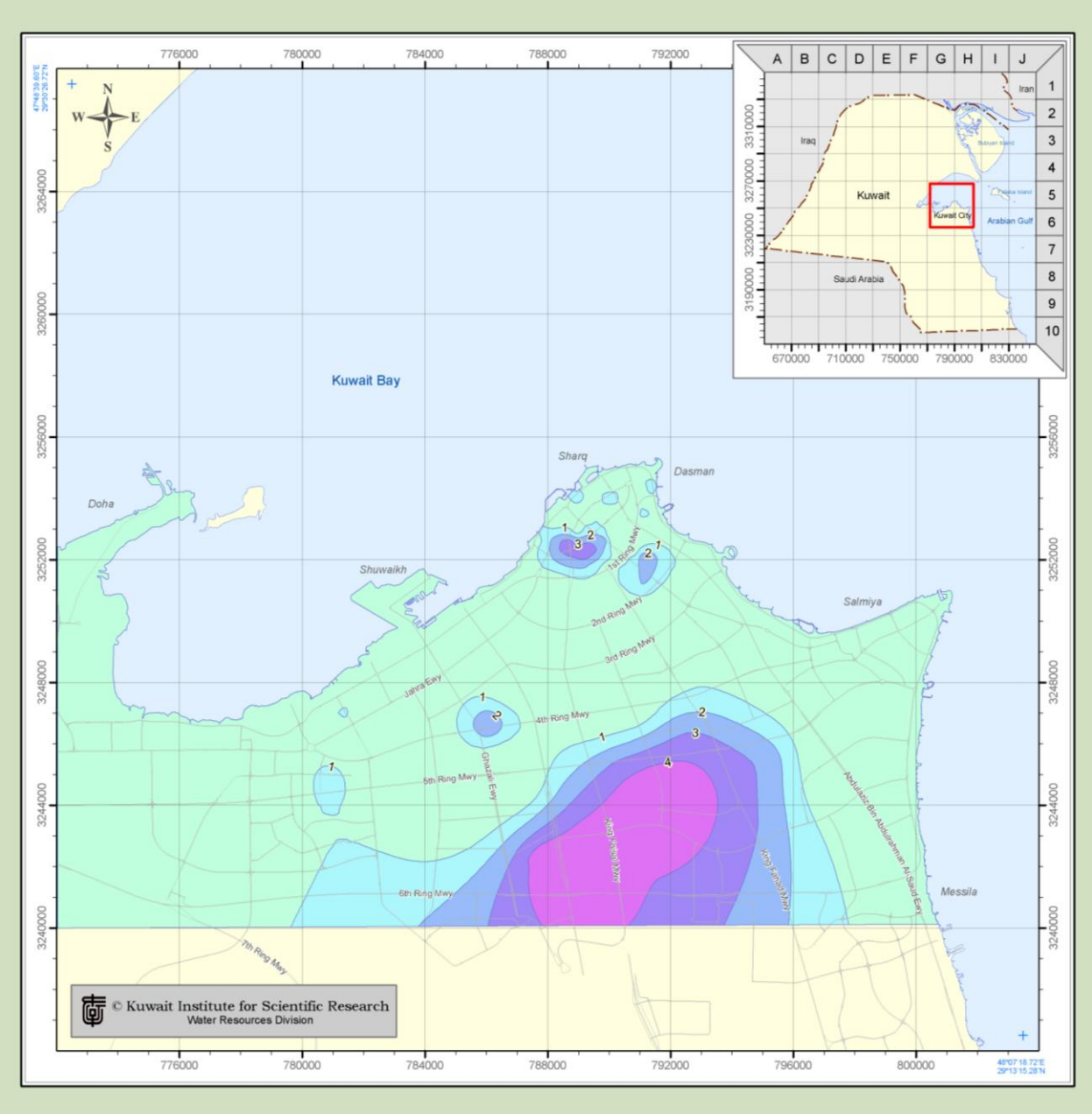

Figure 8. Rise in water level for Kuwait City and suburbs. Contours are water level rise in meters from 1988-2004.

771
772

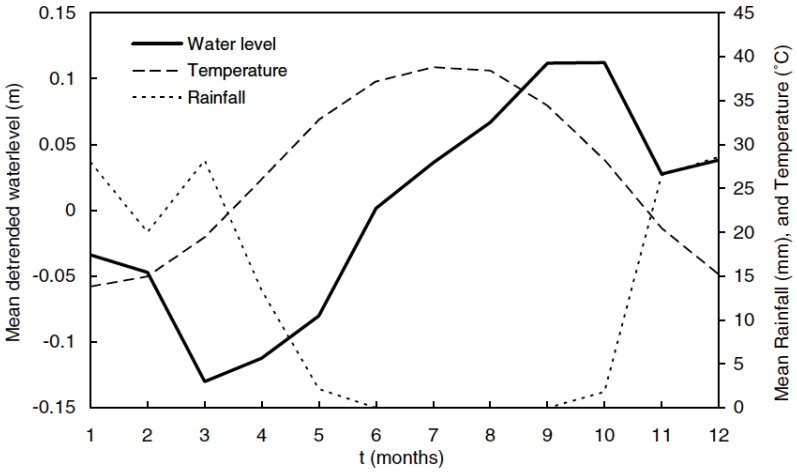

773
774 **Figure 9. Mean variation in groundwater level air temperature, and rainfall for a Kuwait**
775 **City monitoring well–1993-2002 average (reprinted from Almedeij and Al-Ruwaih, 2006).**
776

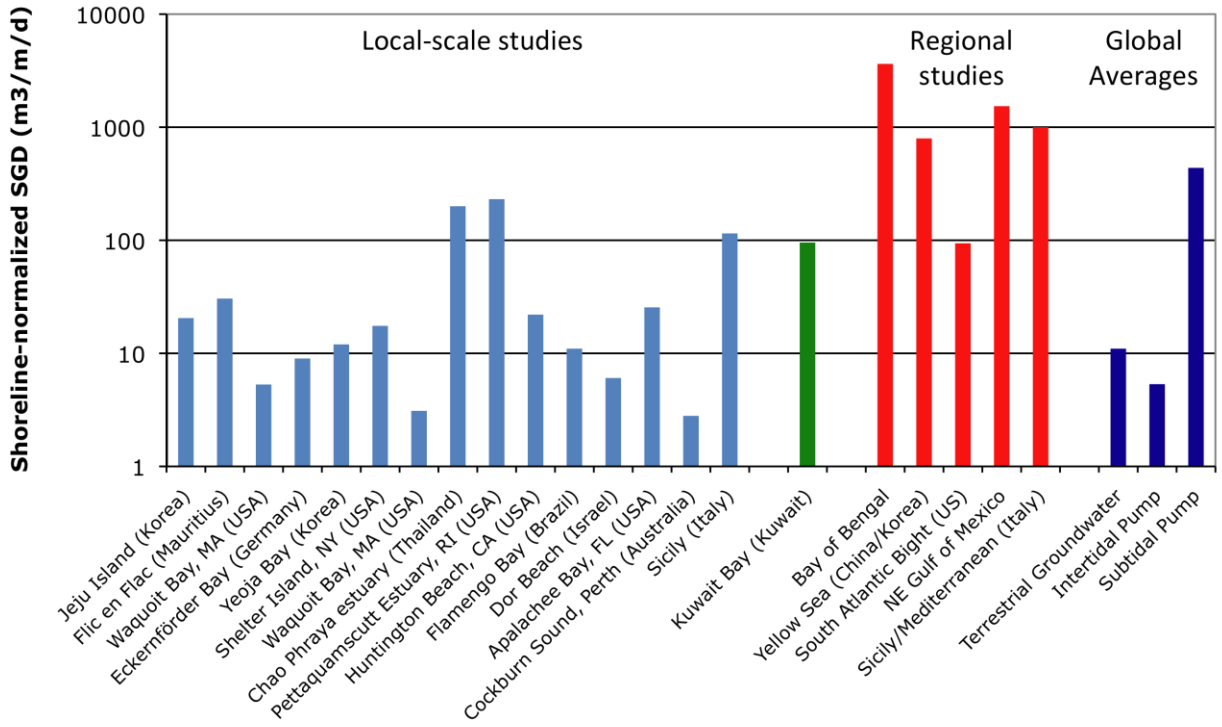

Figure 10. Shoreline-length normalized submarine groundwater discharge for a wide range of global studies including this study. [Reference in order of appearance on figure, L to R: Hwang et al. (2005a); Burnett et al. (2006); Charette et al. (2001); Purkl & Eisenhauer (2004); Hwang et al. (2005b); Dulaiova et al. (2006a); Mulligan and Charette (2006); Dulaiova et al. (2006b); Kelly and Moran (2002); Boehm et al. (2006); Burnett et al. (2006); Swarzenski et al. (2006); Burnett et al. (2002); Burnett et al. (2006); Burnett and Dulaiova (2006); This study; Moore (1997); Kim et al. (2005); Moore (1996); Cable et al. (1996); Moore (2006); Zektser (2000); Riedl et al. (1972); Riedl et al. (1972)].

801
802
803
804
805
806
807
808
809
810

Appendix 1. Darcy's Law calculation for the Kuwait Bay SGD study.

Shoreline segment	Flow path length (m)	Head difference (m)	Gradient	Transmissivity (m^2/d)	Aquifer thickness (m)	Conductivity (m/d)	Velocity (m/d)	Velocity/section (m/d)	Shoreline length (m)	Discharge depth (m)	Dicharge/section (m^3/d)
	7500	10	1.33E-03	175	60	2.92	0.0039				
1	6000	10	1.67E-03	175	60	2.92	0.0049	0.00438	5000	60	1313
2	7000	10	1.43E-03	175	60	2.92	0.0042	0.00451	7500	60	2031
3	5000	10	2.00E-03	175	60	2.92	0.0058	0.00500	8000	60	2400
4	3500	10	2.86E-03	175	60	2.92	0.0083	0.00708	3000	60	1275
5	3500	10	2.86E-03	175	60	2.92	0.0083	0.00833	2500	60	1250
6	8000	10	1.25E-03	175	60	2.92	0.0036	0.00599	9000	60	3234
7	5500	10	1.82E-03	175	70	2.50	0.0045	0.00410	2000	70	573
8	5000	10	2.00E-03	375	80	4.69	0.0094	0.00696	2500	80	1392
9	1000	10	1.00E-02	375	190	1.97	0.0197	0.01456	3000	190	8297
10	7000	10	1.43E-03	175	210	0.83	0.0012	0.01046	9000	210	19776
11	13500	10	7.41E-04	175	210	0.83	0.0006	0.00090	5000	210	949
12	17000	10	5.88E-04	175	210	0.83	0.0005	0.00055	7500	210	872
13	18000	10	5.56E-04	175	210	0.83	0.0005	0.00048	7000	210	701
14	25000	10	4.00E-04	175	210	0.83	0.0003	0.00040	9000	210	753
										sum=	44816

Appendix 2. Radium isotopes and ancillary data for the Kuwait Bay SGD study: surface water samples.

Station ID	Latitude N	Longitude E	EC (mS cm^{-1})	^{223}Ra	^{224}Ra	^{226}Ra	^{228}Ra
				(dpm 100 L^{-1})			
Oct-07							
KBS01	29.3985	48.1836	54.0	0.52	5.4	9.4	23.2
KBS02	29.5038	48.1031	57.1	0.46	10.6	9.7	19.9
KBS03	29.4964	47.9908	57.1	0.39	4.1	7.2	23.6
KBS04	29.4968	47.9022	60.3	0.82	10.3	11.7	32.7
KBS05	29.4328	47.8432	58.2	0.54	3.3	13.1	34.6
KBS06	29.3846	47.7363	55.0	0.64	6.7	18.3	33.1
KBS07	29.3498	47.8645	55.3	0.81	12.0	15.3	38.5
KBS08	29.4143	47.9881	56.0	0.61	7.5	16.4	39.6
KBS09	29.4466	47.9890	56.0	0.39	4.8	21.7	34.4
KBS10	29.3893	48.0998	56.1	0.48	5.1	19.9	39.0
May-08							
KBS01	29.3985	48.1836	31.0	1.05	6.8	6.0	11.3
KBS02	29.5038	48.1031	32.0	0.74	6.3	6.7	10.9
KBS03	29.4964	47.9908	32.0	0.41	3.9	7.4	13.5
KBS04	29.4968	47.9022	32.4	0.72	4.9	6.2	8.3
KBS05	29.4328	47.8432	32.5	0.95	4.1	7.6	12.7
KBS06	29.3846	47.7363	32.0	0.79	10.8	10.2	11.5
KBS07	29.3498	47.8645	33.2	1.66	15.1	7.5	17.6
KBS08	29.4143	47.9881	31.7	0.63	4.2	9.2	17.9
KBS09	29.4466	47.9890	31.8	0.59	2.2	4.0	10.3
KBS10	29.3893	48.0998	31.7	0.32	2.2	4.5	5.2
KBS11	29.3890	47.7783	32.3	0.56	5.0	6.8	10.0
KBS12	29.5509	47.9756	32.5	0.40	7.4	11.1	9.8
KBS13	29.4243	47.9153	32.5	0.78	7.8	8.0	21.5
KBS14	29.4484	48.0528	31.8	0.72	1.1	5.3	13.2
Oct-08							
KBS01	29.3985	48.1836	65.0	1.35	27.0	30.1	62.2
KBS02	29.5038	48.1031	65.0	1.24	17.1	18.0	38.7
KBS03	29.4964	47.9908	63.5	0.74	12.7	24.5	45.1
KBS04	29.4968	47.9022	63.6	1.16	12.0	17.4	36.3
KBS05	29.4328	47.8432	63.5	0.87	12.8	23.8	47.5
KBS06	29.3846	47.7363	63.4	1.16	22.3	24.9	50.0
KBS07	29.3498	47.8645	65.0	0.80	21.3	24.3	46.6
KBS08	29.4143	47.9881	63.7	1.34	14.9	28.1	49.0
KBS09	29.4466	47.9890	63.3	0.85	10.4	46.0	54.8
KBS10	29.3893	48.0998	62.6	0.28	14.1	28.7	60.7
KBS11	29.3890	47.7783	63.7	1.23	20.4	25.3	68.9
KBS12	29.5509	47.9756	63.9	0.37	9.8	18.2	32.5
KBS13	29.4243	47.9153	63.8	1.17	13.1	26.0	57.6
KBS14	29.4484	48.0528	63.2	0.69	10.9	21.9	49.3
Jun-08							
KBS15	28.9245	48.2108	42.90	0.28	6.1	11.0	13.3
KBS16	28.9294	48.2182	42.40	0.52	4.1	13.0	19.9
KBS17	28.9337	48.2275	43.00	0.25	3.0	18.8	18.7
KBS18	28.9382	48.2369	42.90	0.44	3.9	11.2	15.9
KBS19	28.9420	48.2456	43.00	0.11	1.9	19.8	30.0
KBS20	28.9468	48.2543	43.00	0.38	1.2	16.9	24.8
KBS21	28.9532	48.2631	43.20	0.06	0.4	19.0	21.2
KBS22	28.9585	48.2718	43.20	0.31	2.3	13.9	26.8
KBS23	29.6000	48.1642	43.00	0.79	7.8	22.3	40.5

Appendix 3. Radium isotopes and ancillary data for the Kuwait Bay SGD study: groundwater samples.

Station ID	Latitude N	Longitude E	EC (mS cm^{-1})	^{223}Ra	^{224}Ra	^{226}Ra	^{228}Ra
				(dpm 100 L^{-1})			
Oct-07							
KBL01			8.4	7.5	543	991	567
KBL02			68.0	14.6	468	840	1430
KBL03			32.0	35.3	1365	1521	2825
Jan-08							
KBL01	48.1004	29.3469	55.0	8.0	163	88	203
KBL02	48.0727	29.3395	35.9	44.1	6387	677	917
KBL03	48.0587	29.3364	34.4	47.5	2036	580	1702
KBL04	48.0264	29.3566	12.2	9.4	343	28	65
KBL05	48.0215	29.3652	9.6	2.7	77	89	55
KBL07	47.9996	29.3859	67.7	1.5	110	157	154
KBL08	48.0021	29.3855	44.0	1.1	46	129	56
KBL09	47.9903	29.3900	67.0	32.9	737	952	1146
KBL10	47.9881	29.3813	69.5	3.4	61	68	309
KBL11	47.9764	29.3827	46.4	3.7	85	50	145
KBL12	47.9653	29.3733	26.0	1.2	59	42	64
KBL14	47.9086	29.3396	7.0	21.0	759	68	427
KBL15	47.7994	29.3708	54.2	59.4	2349	150	2064
KBL16	47.6883	29.3482	8.8	2.6	131	152	116
KBL16-dup	47.6883	29.3482	8.8	4.6	112	35	176
KBL17	47.7186	29.4215	7.4	6.1	170	231	321
KBL19	47.8957	29.5769	8.6	4.0	195	166	257
KBL20	47.9119	29.6142	12.5	8.4	295	174	404
KBL21	47.9872	29.3253	15.7	20.5	444	131	514
Oct-08							
WRA-1L	47.9900	29.3255	6.7	12.9	246	62	354
WRA-4L	47.9860	29.3212	11.7	11.5	639	141	453
WRA-7L	47.9529	29.3394	8.0	7.0	396	89	297
WRA-5	47.9836	29.3212	6.3	10.4	281	53	230
WRK-1L	47.9684	29.3381	19.8	6.9	527	75	523
WRKH-1L	47.9592	29.3295	13.2	11.0	382	80	457
WRKH-3L	47.9653	29.3230	4.0	5.9	365	115	473
WRK-2	47.9598	29.3352	15.2	22.2	729	287	1270
WRKH-2L	47.9592	29.3244	10.7	20.0	539	137	465
KBL - 17	47.7186	29.4215	8.5	1.9	96	35	77
KBL - 19	47.8957	29.5769	9.2	1.8	77	26	91
KBL - 20	47.9119	29.6142	13.3	2.7	187	80	180
KBL - 21	47.9872	29.3253	18.3	7.1	260	71	248
KBL - 26			8.0	1.2	88	34	217
KBL - 28			8.1	0.9	72	40	88
KBL - 29			16.2	6.7	237	129	154
KBL - 30			15.5	6.6	209	58	309
KBL - 31			103.5	21.9	811	192	927
KBL - 01	48.1004	29.3469	61.3	81.3	3	63	162
KBL - 03	48.0587	29.3364	33.5	698.0	15	303	918
KBL - 04	48.0264	29.3566	12.0	42.0	1	15	16
KBL - 05	48.0215	29.3652	5.3	52.7	2	73	71
.BL - 07(A&I	47.9996	29.3859	75.3	192.2	4	109	500
KBL - 08	48.0021	29.3855	24.9	42.1	1	39	168
KBL - 09	47.9903	29.3900	43.7	1096.0	31	1221	1097
.BL - 10(A&I	47.9881	29.3813	124.2	69.8	2	40	156
.BL - 11(A&I	47.9764	29.3827	80.5	72.7	4	34	121
KBL - 12	47.9653	29.3733	25.8	48.2	1	48	131
KBL - 14	47.9086	29.3396	31.0	1147.6	26	107	1964
KBL - 15	47.7994	29.3708	71.5	1680.5	23	123	1710
KBL - 16	47.6883	29.3482	9.4	81.2	1	19	81
KBL - 22			9.4	172.9	4	77	255
KBL - 23			82.6	105.4	2	21	89
KBL - 24			9.2	94.9	2	27	91
KBL - 25			7.0	191.9	3	45	215
KBL - 27			10.7	176.2	3	33	203